

## Helium Production Analysis of Nickel-based Alloy in Molten Salt Reactor

Bo Zhou<sup>a,b</sup>, Yang Zou<sup>a,b\*</sup>, Rui Yan<sup>a,b</sup>, Pu Yang<sup>a,b</sup>, Minghai Li<sup>a,b</sup>, Ye Dai<sup>a,b</sup>, Yafen Liu<sup>a,b</sup>, Shihe Yu<sup>a,b</sup>, Zhijun Li<sup>a,b</sup>

<sup>a</sup>Shanghai Institute of Applied Physics(CAS), Jia Luo Road, Jia Ding District Shanghai, China 201800;

<sup>b</sup>Key Laboratory of Nuclear Radiation and Nuclear Energy Technology, Chinese Academy of Science, Shanghai, China 201800.

\*Corresponding author: [zouyang@sinap.ac.cn](mailto:zouyang@sinap.ac.cn)

### 1. Introduction

As a candidate of the Generation IV reactor[1], latest research of molten salt cooled reactor is focused on distinct advantage of high temperature and low pressure of the main coolant circuit. Compared with the traditional pressurized water reactor, molten salt cooling system with high temperature and low pressure can take the heat out of the core more effectively with higher security [2-4]. At the same time, it brought a bigger challenge for the primary circuit pressure boundary material, which requires good corrosion and radiation resistance and high temperature resistant. Pebble bed-Fluoride salt-cooled High temperature Reactor (PB - FHR) also is a new type of molten salt cooled reactor [5,6], which has good performance in terms of safety and economy. Fuel pebble can withstand the maximum temperature 1600 °C, and it can maintain integrity, which ensures the radionuclide will not spread out from the fuel pellets in case of all possible accident. TMSR-SF1 is one of the research targets of Chinese academy of sciences. The fuel and coolant type in TMSR-SF1 is similar to PB-FHR. Hastelloy-N alloy is one kind of nickel base alloy that was chose for the primary circuit pressure boundary alternative material in TMSR-SF1 system.

In TMSR-SF1, the helium can formed by neutron-capture transmutation, it can form bubbles and void cavities [7], and accelerate the onset of void welling. The performance such as corrosion resistance and high temperature resistant of the material will reduced [8-10]. The production rates of helium depending on the neutron energy spectrum and flux which has great difference due to different locations in core. So the main source and production of the helium with various conditions need to be quantitatively analyzed for TMSR-SF1.

### 2. The source of the helium produced

The 10MW TMSR-SF1 is a graphite moderated FLiBe salt-cooled reactor using spherical fuel elements (6cm in diameter) with TRISO coated particles(enrichment of <sup>235</sup>U is 17.08%). Operating temperature is between 600 °C and 650 °C and the core dimensions is 2.6m (dia.) \* 3.0m (h). The primary loop pipe and the corresponding pressure boundary materials, such as the main container, safe containers, control rod guide, etc. are all of the Hastelloy-N alloys. Most of the elements in nickel base alloy can produce helium by (n,α) reactions with neutron energy above ~4MeV. The main source from such reaction is the five kinds of nickel natural isotopes

especially from <sup>58</sup>Ni. Other elements in Hastelloy-N alloy have much smaller contribution for helium production.

Another significant source for helium production is <sup>58</sup>Ni (n,r) <sup>59</sup>Ni (n,α) two steps reaction. It is known that <sup>59</sup>Ni is a kind of artificial radionuclide that is not found in natural nickel element. The main reaction type and cross section with neutron for five isotopes of natural nickel and <sup>59</sup>Ni is as shown in Table I . Note that <sup>59</sup>Ni has a higher thermal neutron (n,α) cross section compared to five isotopes of natural nickel. This contribution becomes the major source of helium in Hastelloy-N alloy.

Table I . Main Reaction Cross Section of Isotopes of Nickel

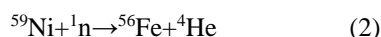
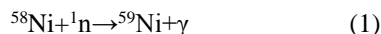
Isotopes	Natural abundance /%	Reaction type	Cross section/barn	Product
<sup>58</sup> Ni	68.27	(n, α)	2.01E-05	<sup>55</sup> Fe
		(n, γ)	1.65	<sup>59</sup> Ni
<sup>59</sup> Ni	0	(n, α)	5.44	<sup>56</sup> Fe
		(n, γ)	23.6	<sup>60</sup> Ni
<sup>60</sup> Ni	26.10	(n, α)	8.22E-06	<sup>57</sup> Fe
		(n, γ)	0.935	<sup>61</sup> Ni
<sup>61</sup> Ni	1.134	(n, α)	8.10E-06	<sup>58</sup> Fe
		(n, γ)	0.977	<sup>62</sup> Ni
<sup>62</sup> Ni	3.593	(n, α)	3.55E-07	<sup>59</sup> Fe
		(n, γ)	5.80	<sup>63</sup> Ni
<sup>64</sup> Ni	0.904	(n, α)	4.58E-08	<sup>61</sup> Fe
		(n, γ)	0.579	<sup>65</sup> Ni

In TMSR-SF1, there are two other sources, which is <sup>10</sup>B(n,α), and <sup>6</sup>Li(n,α). Although it has higher (n,α) cross section for <sup>6</sup>Li in thermal reactor, it has lower abundance

of natural lithium, which is about ~7%. And lithium is not the main impurity of the Hastelloy-N alloy.

### 3. Method and theory

Two step physical processes for helium production of  $^{58}\text{Ni}$  are as follows:



The corresponding differential equation expression of the concentration for  $^{58}\text{Ni}$ ,  $^{59}\text{Ni}$  and  $^4\text{He}$  is as follows:

$$\frac{dN_{58}(t)}{dt} = -N_{58}(t) \cdot \phi \cdot (\sigma(n, \gamma)_{ni58} + \sigma(n, a)_{ni58} + \dots) \quad (3)$$

$$\begin{aligned} \frac{dN_{59}(t)}{dt} &= N_{58}(t) \cdot \phi \cdot \sigma(n, \gamma)_{ni58} \\ &- N_{59}(t) \cdot \phi \cdot (\sigma(n, \gamma)_{ni59} + \sigma(n, p)_{ni59} + \sigma(n, \alpha)_{ni59}) - \lambda N_{59}(t) \end{aligned} \quad (4)$$

$$\frac{dHe(t)}{dt} = N_{58}(t) \cdot \phi \cdot \sigma(n, a)_{ni58} + N_{59}(t) \cdot \phi \cdot \sigma(n, a)_{ni59} \quad (5)$$

$N_{58}(t)$ ,  $N_{59}(t)$ ,  $He(t)$  respectively is the function of atomic density change over time.  $\Phi$  and  $\sigma$  is the neutron flux and cross section respectively. Corner mark of  $\sigma$  is on behalf of the corresponding nuclide.

Physical process for helium production of  $^{10}\text{B}$  is as follows:



The corresponding differential equations of the concentration for  $^{10}\text{B}$  and  $^4\text{He}$  are ignored here.

### 4. Calculation results

#### 4.1 Neutron flux and cross section parameters

Monte-carlo program of SCALE6.1 has been applied to model and the neutron flux and energy spectrum of TMSR is calculated. The model of the core with thermal power of 10 MW in the conceptual design stage is shown in Fig. 1, the evaluated neutron cross section that was used for  $^{58}\text{Ni}$ ,  $^{59}\text{Ni}$  and  $^{10}\text{B}$  is shown on Fig.2 and Fig.3.

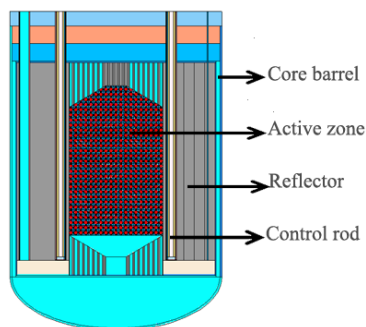


Fig.1. Model of the core

The cross section has different characteristics for each nuclide and each reaction type. So, three different locations were selected along the radial direction of the core for neutron flux and effective cross section calculation. Neutron spectrum and the corresponding cross section for different locations in core are shown in Fig. 4 and Table II. The result showed that the neutron

spectrum has a great difference at three different locations and the total flux and cross section is differed by more than 97% and 48% respectively.

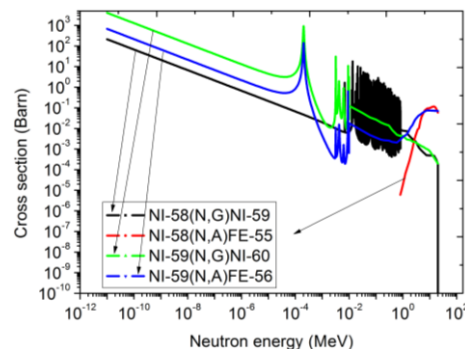


Fig.2. Evaluated neutron cross section for  $^{58}\text{Ni}$ ,  $^{59}\text{Ni}$

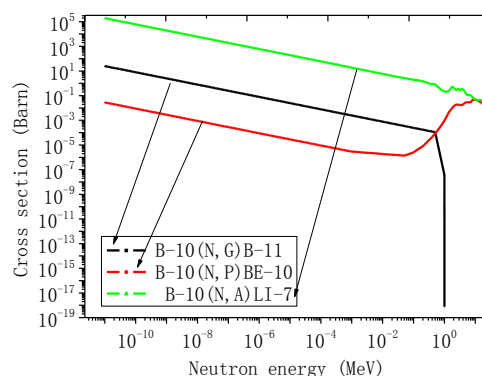


Fig. 3. Evaluated Neutron cross section for  $^{10}\text{B}$

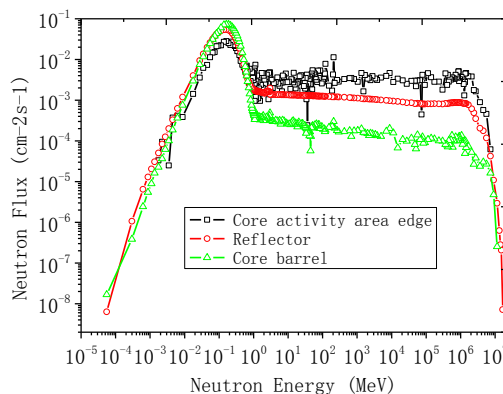


Fig. 4. Neutron spectrum in core

Table II. Neutron flux and Effective Cross Section

Parameter for three locations		Active zone edge	Reflector	Core barrel
Flux/cm <sup>2</sup> s <sup>-1</sup>		4.55E+13	1.52E+13	1.14E+12
Cross section /barn	$^{10}\text{B} (n, \alpha)$	934.2	1602	1664
	$^{58}\text{Ni} (n, \gamma)$	1.025460	1.76	1.83
	$^{58}\text{Ni} (n, \alpha)$	2.19E-04	5.16E-05	1.02E-05
	$^{59}\text{Ni} (n, \alpha)$	4.0087	5.89	5.95
	$^{59}\text{Ni} (n, \gamma)$	23.58	34.8	35.1

## 4.2 Helium production

### 4.2.1 Nickel's contribution

Fig. 5 shows the  $^{58}\text{Ni}$  and  $^{59}\text{Ni}$  concentration as a function of Irradiation time at the edge of active zone. The concentration of  $^{59}\text{Ni}$  constantly accumulated without reaching equilibrium over a long time range from 1s to about several years. Fig. 6 shows the calculated helium production from both the  $^{58}\text{Ni}$  ( $n,\alpha$ ) reaction and  $^{58}\text{Ni}(n,\gamma)^{59}\text{Ni}$  ( $n,\alpha$ ) reaction. It can be seen from the results that 10 days before,  $^{59}\text{Ni}$  is gradually accumulated and helium is mainly produced from the  $^{58}\text{Ni}(n,\alpha)$  reaction. After 10 days, the two-step  $^{58}\text{Ni}(n,\gamma)^{59}\text{Ni}(n,\alpha)$  reactions become dominated for helium production.

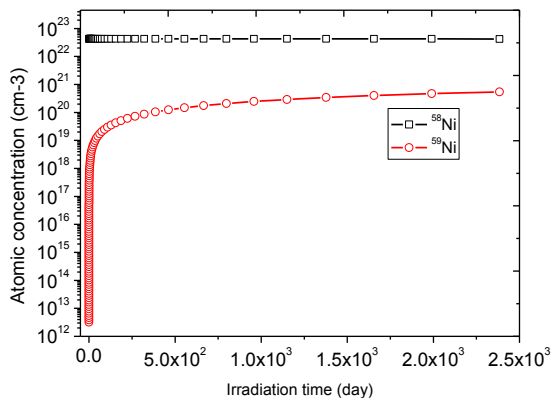


Fig. 5. Concentration of  $^{58}\text{Ni}$  and  $^{59}\text{Ni}$  during irradiation

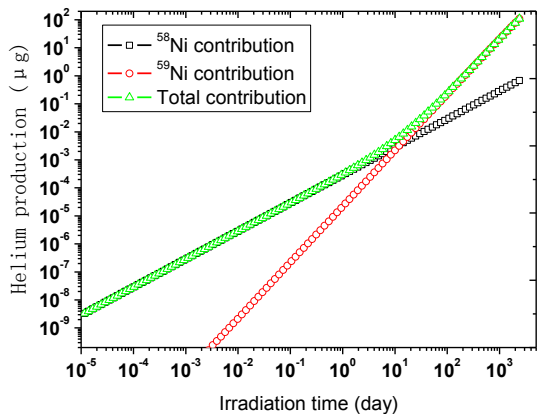


Fig. 6. Helium production comparison from  $^{58}\text{Ni}$  ( $n,\alpha$ ) and  $^{58}\text{Ni}(n,r)^{59}\text{Ni}$  ( $n,\alpha$ ) reactions

Calculation results for different location are shown in Fig. 6. During the irradiation time, the gradually accumulated amount of helium did not reach saturation concentration, and the calculation results for various locations of the core is several orders of magnitude different due to the distinctive energy spectrum and flux. In order to get saturated flux, helium production with different flux was calculated, the results are shown as a function of the thermal neutron flux in Fig. 8, showing that the helium saturation total flux for nickel is about  $6.6 \cdot 10^{24} \text{cm}^{-2}$  ( $\pm 10\%$ ).

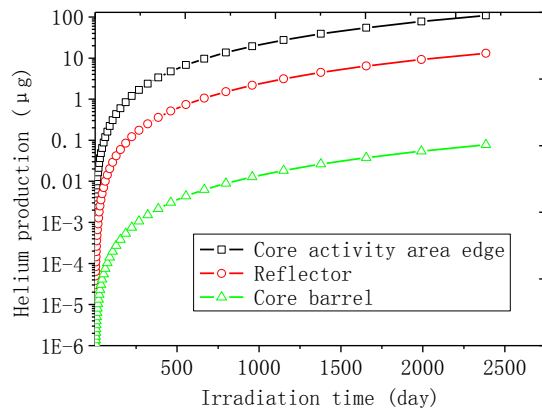


Fig. 7. Helium production of in core ( $^{58}\text{Ni}$ )

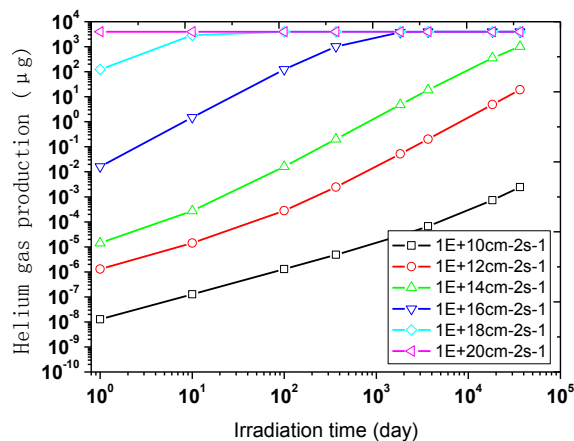


Fig. 8. Helium concentrations as a function of the neutron flux ( $^{58}\text{Ni}$ )

### 4.2.2 Boron's contribution

The helium production for boron was calculated at different locations and different flux with the similar method applied to nickel, which is shown in Fig. 9 and Fig. 10. The results show that, helium saturation flux for boron is  $9.38 \cdot 10^{21} \text{cm}^{-2}$  ( $\pm 10\%$ ) due to the larger cross section of boron.

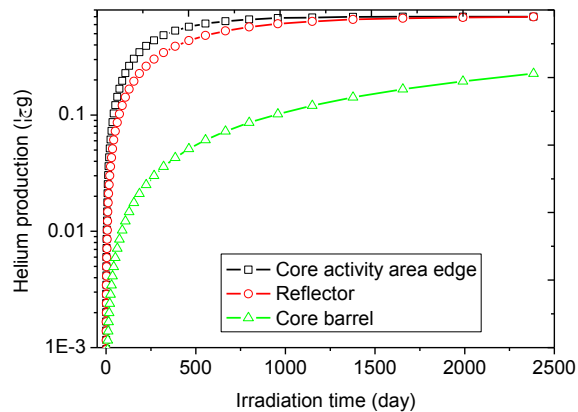


Fig.9. Helium production in core ( $^{10}\text{B}$ )

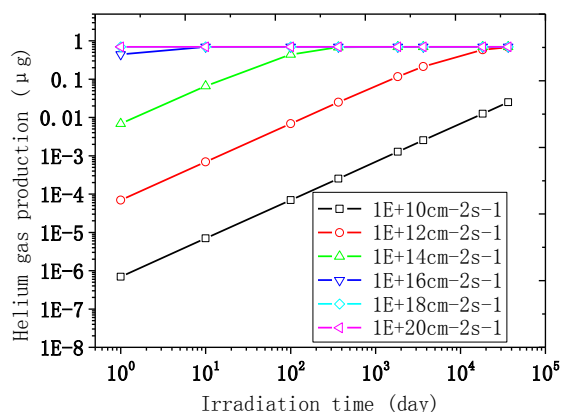


Fig.10. Helium production with different Neutron flux (<sup>10</sup>B)

## 5. Conclusions

The two-step nickel reaction  $^{58}\text{Ni}(n,\gamma)^{59}\text{Ni}(n,\alpha)$  can produce high levels of helium, which playing a dominant role for helium production of Hastelloy-N alloy in molten salt reactor. It is worth noting that this reaction is non-linear with exposure due to the buildup of  $^{59}\text{Ni}$ . Therefore, this contribution shows a delay in its production and continuously accelerates in rate with increasing exposure, only saturating at neutron total flux of  $6.6 \times 10^{24} \text{cm}^{-2} (\pm 10\%)$ . It is important that, the degree of acceleration is directly depends on the neutron flux and neutron spectrum, which vary strongly with different position in cores. Annual maximum production of helium per volume is roughly  $3 \mu\text{g} (\pm 10\%)$  in TMSR-SF1.

## Acknowledgements

This work is supported by the “Strategic Priority Research Program” of the Chinese Academy of Sciences, Grant No. XDA02010200.

## References

- [1] Rosenthal MW, Briggs RB, Haubenreich PN, “*Molten-salt reactor program*,” ORNL report No. ORNL-4832, Oak Ridge, TN, US. (1972).
- [2] Uhlir J, “Chemistry and technology of molten salt reactors – history and perspectives,” *Nucl. Mater.* **360**, 6–11 (2007).
- [3] LeBlanc D, “Molten salt reactors: a new beginning for an old idea,” *Nucl. Eng. Des.* **240**, 1644–1656 (2010).
- [4] Greene SR, et al., “Pre-Conceptual Design of a Fluoride-Salt-Cooled Small Modular Advanced High-Temperature Reactor (SmAHTR),” ORNL/TM - 2010/199, Oak Ridge National Laboratory, Oak Ridge, TN, US(2010).
- [5] Raluca OS, Per FP, “The current status of fluoride salt cooled high temperature reactor (FHR) technology and

- its overlap with HIF target chamber concepts” *Nucl. Instrum. Methods Phys. Res., Sect. A.*, **733** 57–64(2014).
- [6] Guifeng Z, Yang Z, Hongjie X, “Basic neutron physical parameters study on thorium using in pebble bed fluoride salt-cooled high temperature reactor” *Nucl. Power Eng.* (2014).
  - [7] Dai Y, Odette GR, Yamamoto T, “The effect of helium in irradiated structural alloys,” *Nucl. Mater.*, **1**, 141-193(2012).
  - [8] LeBlanc D, “Molten salt reactors: a new beginning for an old idea,” *Nucl. Eng. Des.* **240**, 1644–1656 (2010).
  - [9] Ouyang FY, Chang CH, You BC, Yeh TK, Kai JJ, “Effect of moisture on corrosion of Ni-based alloys in molten alkali fluoride FLiNaK salt environments,” *J. Nucl. Mater.* **437**, 201–207 (2013).
  - [10] Murty KL, Charit I, “Structural materials for Gen-IV nuclear reactors: challenges and opportunities,” *J. Nucl. Mater.* **383**, 189–195 (2008).